



Published in final edited form as:

Cell Rep. 2015 September 8; 12(10): 1606–1617. doi:10.1016/j.celrep.2015.07.058.

TMC1 and TMC2 Localize at the Site of Mechanotransduction in Mammalian Inner Ear Hair Cell Stereocilia

Kiyoto Kurima^{1,*}, Seham Ebrahim^{2,*}, Bifen Pan³, Miloslav Sedlacek², Prabuddha Sengupta⁴, Bryan A. Millis², Runjia Cui², Hiroshi Nakanishi¹, Taro Fujikawa², Yoshi Kawashima¹, Byung Y. Choi¹, Kelly Monahan¹, Jeffrey R. Holt³, Andrew J. Griffith¹, and Bechara Kachar²

¹Molecular Biology and Genetics Section, National Institute on Deafness and Other Communication Disorders, National Institutes of Health, Bethesda, Maryland, 20892, USA

²Laboratory of Cell Structure and Dynamics, National Institute on Deafness and Other Communication Disorders, National Institutes of Health, Bethesda, Maryland, 20892, USA

³Department of Otolaryngology, F.M. Kirby Neurobiology Center, Boston Children's Hospital, Harvard Medical School, Boston, MA 02115, USA

⁴Cell Biology and Metabolism Program, Eunice Kennedy Shriver National Institute of Child Health and Human Development, Bethesda, MD 20892

Summary

Mechanosensitive ion channels at stereocilia tips mediate mechanoelectrical transduction (MET) in inner ear sensory hair cells. Transmembrane channel-like 1 and 2 (TMC1 and TMC2) are essential for MET and are hypothesized to be components of the MET complex, but evidence for their predicted spatiotemporal localization in stereocilia is lacking. Here we determine the stereocilia-localization of the TMC proteins in mice expressing TMC1-mCherry and TMC2-AcGFP. Functionality of the tagged proteins was verified by transgenic rescue of MET currents and hearing in *Tmc1*^{-/-}; *Tmc2*^{-/-} mice. TMC1-mCherry and TMC2-AcGFP localize along the length of immature stereocilia. However, as hair cells develop, the two proteins localize

Correspondence: Bechara Kachar 35A Convent Drive, Room 3D824. Laboratory of Cell Structure and Dynamics. National Institute on Deafness and Other Communication Disorders, National Institutes of Health, Bethesda, Maryland, 20892, Phone : 301-402-1600 Kacharb@nidcd.nih.gov. Andrew J. Griffith 35A Convent Drive, Room GF103. Molecular Biology and Genetics Section. National Institute on Deafness and Other Communication Disorders, National Institutes of Health, Bethesda, Maryland, 20892, Phone : 301-402-2829 Griffita@nidcd.nih.gov.

*Contributed equally

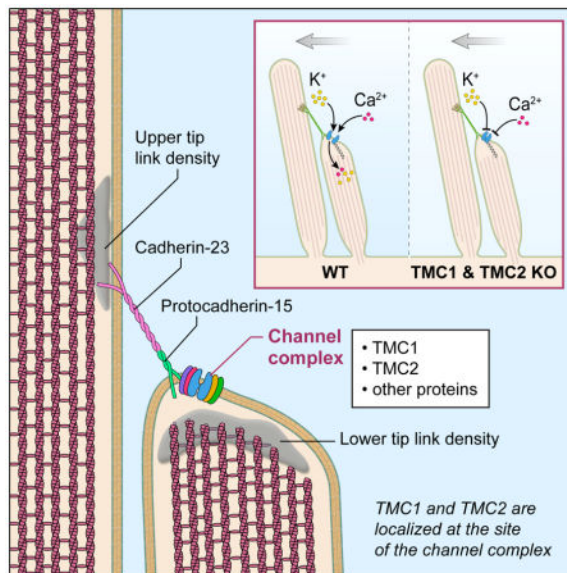
Author Contributions

K.K. conceived, designed and generated transgenic mice, collected and analyzed data. S.E. collected and analyzed data. B.P. collected and analyzed conventional MET electrophysiology data. M.S. collected and analyzed electrophysiology data acquired with fluid jet stimulation. B.M. helped acquire confocal microscope images. P.S. helped with analyzes and quantification of fluorescence data. R.C., H.N., T.F., Y.K. helped collecting data. B.Y.C. and K.M. helped generate transgenic mice. J.R.H. analyzed conventional MET data. A.J.G. conceived and designed transgenic mice. S.E. and B.K. conceived and designed localization experiments, collected and analyzed data. K.K., P.S., and B.K. generated the figures, and K.K., S.E., A.J.G. and B.K. wrote the paper. All authors provided comments and approved the final submission of the manuscript.

Publisher's Disclaimer: This is a PDF file of an unedited manuscript that has been accepted for publication. As a service to our customers we are providing this early version of the manuscript. The manuscript will undergo copyediting, typesetting, and review of the resulting proof before it is published in its final citable form. Please note that during the production process errors may be discovered which could affect the content, and all legal disclaimers that apply to the journal pertain.

predominantly to stereocilia tips. Both TMCs are absent from the tips of the tallest stereocilia, where MET activity is not detectable. This distribution was confirmed for the endogenous proteins by immunofluorescence. These data are consistent with TMC1 and TMC2 being components of the stereocilia MET channel complex.

Graphical Abstract



Introduction

Mechano-electrical transduction (MET), whereby mechanical stimuli are converted to electrical signals, is an integral property of inner ear hair cells, accomplished by their mechanosensory organelle, the stereocilia hair bundle. Each bundle comprises dozens of actin-based protrusions with graded lengths, organized in a staircase array. Tip links, extracellular protein filaments composed of cadherin-23 (CDH23) and protocadherin-15 (PCDH15), connect pairs of adjacent stereocilia near their tips in the direction of optimal mechanosensitivity of the bundle (Kazmierczak et al., 2007; Sakaguchi et al., 2009). At each end of the tip link are densely packed macromolecular complexes underlying the stereocilia membrane, known as tip link insertion plaques. The upper insertion plaque is presumed to contain a cluster of motor proteins (Grati and Kachar, 2011) that maintains a resting tension on the tip link (Schwander et al., 2010). The lower tip link insertion site is thought to be the site for the MET channel complex (Beurg et al., 2009). Stereocilia-mediated MET occurs as a consequence of stereocilia bundle deflection towards the tallest row of stereocilia, which exerts tension on tip links, opening MET channels and causing depolarization of the hair cell. The developmental acquisition of MET, which has been spatiotemporally characterized in rat (Waguespack et al., 2007) and mouse (Lelli et al., 2009) is tonotopic, with onset of MET in hair cells in the organ of Corti between postnatal day (P) 1 and P2, and fully mature MET being reached by P8.

Aside from the tip link proteins, the molecular composition of the MET apparatus remains elusive (Fuchs, 2015; Gillespie et al., 2005). The tetraspanin TMHS/LHFPL5 (Beurg et al., 2015; Xiong et al., 2012) and a protein with two transmembrane domains, TMIE (Zhao et al., 2014), have recently been identified as MET channel accessory components. However, the precise spatiotemporal localization of these proteins and the identities of the pore-forming units and other essential auxiliary elements are yet to be determined. Two members of the transmembrane-channel like (TMC) family, TMC1 and TMC2, are candidates to be part of the MET complex based on several lines of evidence: (1) *Tmc1* and *Tmc2* mRNA are selectively expressed in developing hair cells at the onset of acquisition of mechanosensitivity (Kawashima et al., 2011); (2) mutations of *TMC1* cause deafness in humans and mice (Kurima et al., 2002; Vreugde et al., 2002); (3) in the absence of both functional TMC1 and TMC2, hair cells of the mouse auditory and vestibular system lack mechanosensory responses to forward deflection of the hair bundle (Beurg et al., 2014; Kawashima et al., 2011); (4) TMC1- and TMC2-deficient hair cells fail to take up FM1-43 or gentamicin (Kawashima et al., 2011), which enter wild type hair cells via the MET channel (Gale et al., 2001; Marcotti et al., 2005); (5) transient exogenous expression of either TMC1 or TMC2 restored mechanosensitivity in hair cells from double homozygous null mice (*Tmc1*^{-/-}; *Tmc2*^{-/-}), demonstrating that these proteins are necessary for generating MET currents (Kawashima et al., 2011); (6) fish and mouse orthologs of the cytoplasmic domain of PCDH15 were recently shown to interact with both TMC1 and TMC2 (Maeda et al., 2014); (7) a more recent study shows interactions between PCDH15 as well as the MET protein LHFPL5 with TMC1 and TMC2 (Beurg et al., 2015).

While these data collectively suggest that TMC1 and TMC2 are crucial for the development and gating of MET currents (Kawashima et al., 2014), to ascertain whether they are indeed components of the MET complex, it is necessary to verify their localization at the site of the MET channel complex, at the lower tip link insertion sites on shorter stereocilia, from the early postnatal period onward (Beurg et al., 2009). Previous studies reported targeting of fluorophore-tagged TMC1 and TMC2 to the apex of all stereocilia when exogenously expressed using biolistic gene-gun mediated transfection of hair cells cultured *in vitro* (Kawashima et al., 2011) and Beurg et al. (2015) localized TMC1 to stereocilia and kinocilium using antibody labeling. However, a definitive conclusion on the precise spatiotemporal localization of the proteins during postnatal development was precluded by the transient nature of the protein expression, the likelihood of overexpression due to the non-native promoter used, and potential for cell damage by the gene gun method. We addressed this in the current study by generating and characterizing transgenic mice that express TMC1-mCherry and TMC2-AcGFP under their native promoters. We first verified that the fluorophore-tagged TMC proteins mimic the function of the native TMC proteins, by confirming rescue of hearing and vestibular deficits, as well as hair cell MET, in *Tmc1*^{-/-}; *Tmc2*^{-/-} mice expressing TMC1-mCherry and TMC2-AcGFP. Using high performance confocal microscopy we show that both TMC1-mCherry and TMC2-AcGFP localize to the presumed site of MET at stereocilia tips. The pattern of localization of the fluorophore-tagged TMC proteins in the transgenic mice was further validated by immunofluorescence localization of the native proteins using specific anti-TMC1 and -TMC2 antibodies. Finally, we also examined the relationship of TMC1 and TMC2 to the

recently described non-canonical, reverse polarity mechanosensitive currents elicited after disruption of conventional MET (Barr-Gillespie and Nicolson, 2013; Kim et al., 2013; Marcotti et al., 2014).

Results

Generation of TMC1 and TMC2 BAC (bacterial artificial chromosome) transgenic mice

To visualize TMC proteins in hair cells, we generated transgenic mice expressing TMC1 or TMC2 fused to fluorophore tags at their C-termini. The transgenes were derived from BACs encoding mouse genomic *Tmc1* or *Tmc2* to mimic endogenous expression. The native stop codons were replaced with cDNA encoding mCherry or AcGFP, respectively (Figure 1A). We obtained four founder lines segregating *Tmc1-mCherry* and four founder lines segregating *Tmc2-AcGFP*. Using quantitative PCR (qPCR) we estimated that the transgene copy numbers for *Tmc1-mCherry* lines 1, 2, 3 and 4 were 3, 7, 7 and 18, respectively; transgene copy numbers for *Tmc2-AcGFP* lines 1, 2, 3 and 4 were 2, 3, 3 and 5 respectively. To determine whether the TMC1-mCherry and TMC2-AcGFP were functional and could substitute for the function of native TMC1 and TMC2 *in vivo*, each transgenic founder line was crossed with the previously described null *Tmc1*^{-/-}, *Tmc2*^{-/-}, and *Tmc1*^{-/-};*Tmc2*^{-/-} lines (Kawashima et al., 2011). All transgenic mice were fertile on the *Tmc1*^{-/-};*Tmc2*^{-/-} background and transmitted the transgenes to offspring. In *Tmc1-mCherry* line 3, however, transmission of the transgene through males was restricted to female offspring, indicating X-chromosome integration of the transgene in this line.

Functional evaluation of TMC1-mCherry and TMC2-AcGFP

Fluorophore tags may alter the configuration of proteins to which they are appended. To evaluate the functionality of TMC1-mCherry, we recorded auditory brainstem response (ABR) threshold measurements from transgenic mice from founder lines 1, 2 or 4 segregating *Tmc1-mCherry* on a *Tmc1*^{-/-} background. *Tmc1*^{-/-} mice are profoundly deaf, but we determined that hearing in these mice was fully rescued when *Tmc1-mCherry* was present (Figure 1B), indicating that the mCherry-tagged TMC1 can replace the native protein without detectable changes in auditory function. No difference was observed in the ABR thresholds among the different *Tmc1-mCherry* founder lines despite differences in transgene copy number, suggesting that the targeting and function of TMC1 is not significantly affected by gene dosage. Only partial rescue of auditory function was observed in females from line 3 (Figure 1B), where the *Tmc1-mCherry* transgene segregated in a pattern consistent with X-linked inheritance (Lyon, 1961). The presence of *Tmc2-AcGFP* did not rescue hearing in *Tmc1*^{-/-} mice (Figure 1B), consistent with previous reports on the inability of TMC2 to compensate for lack of TMC1 in the mature auditory system (Kawashima et al., 2011). Finally, the abnormal motor vestibular phenotypes, including head-bobbing and arching, present in *Tmc1*^{-/-};*Tmc2*^{-/-} mice (Kawashima et al., 2011), were not detected when either *Tmc1-mCherry*, or *Tmc2-AcGFP* or both transgenes were present (data not shown). This rescue of function indicates that the fluorophore tags did not significantly affect the function of TMC1 or TMC2 in the vestibular system, and that either TMC1 or TMC2 are sufficient to restore function in the vestibular system.

We next investigated the effects on whole-cell MET currents when native TMC1 or TMC2 were replaced with fluorophore-tagged TMC1 or TMC2. As previously reported, inner hair cells (IHCs) and outer hair cells (OHCs) from *Tmc1*^{-/-};*Tmc2*^{-/-} mice have no detectable MET currents (Kawashima et al., 2011). We recorded whole-cell MET currents from IHCs and OHCs of *Tmc1*^{-/-};*Tmc2*^{-/-} mice expressing either *Tmc1-mCherry* (line 2), *Tmc2-AcGFP* (line 3), or both transgenes, in developing (P3) and mature (P7) stereocilia (Figure 1C). At P3, we observed partial rescue of MET currents in both OHCs and IHCs in the presence of *Tmc1-mCherry*, or *Tmc2-AcGFP* (Figure 1C). When both transgenes were present a small but statistically significant ($p=0.03$) difference in MET currents was observed between IHCs of wild type and the *Tmc1+2* BAC groups, but no significant difference ($p=0.50$) was seen between OHCs of the two groups. At P7, the effects of transgene expression differed between IHCs and OHCs: In OHCs, the presence of *Tmc1-mCherry* restored MET currents, but the presence of *Tmc2-AcGFP* did not. The partial rescue of MET currents by *Tmc2-AcGFP* at P3 but not at P7 is consistent with the previously reported decline in *Tmc2* mRNA levels in cochlear hair cells after early postnatal increase (Kawashima et al., 2011), indicating an agreement between spatiotemporal expression patterns of the transgenes in rescued mice and the endogenous genes in wild type mice. The data also support the hypothesis that, when it is expressed, TMC2 is able to partially compensate for TMC1 function (Kawashima et al., 2011). In IHCs at P7, however, the presence of either *Tmc1-mCherry* or *Tmc2-AcGFP* resulted in partial recovery of MET currents, and expression of both transgenes resulted in a complete recovery (Figure 1C). This suggests that *Tmc2* expression does not decline in IHC to the extent that it does in OHC between P3 and P7. Collectively, these results show that the *Tmc1-mCherry* and *Tmc2-AcGFP* transgenes can restore MET function and normal ABR thresholds in *Tmc1*^{-/-};*Tmc2*^{-/-} mice, and that different transgene copy numbers appear to have no significant effect on MET function or ABR thresholds.

Localization of TMC1

In *Tmc1-mCherry* mice on a *Tmc1*^{-/-} background we observed mCherry fluorescence in the form of diffraction-limited puncta in stereocilia of auditory and vestibular hair cells (Figure 2A–D). The presence of discrete puncta, rather than a uniform diffuse fluorescence along the stereocilia, indicates an enrichment of a few closely associated TMC1 molecules in small clusters within each punctum. In cochlear hair cells at P8 (Figure 2A and 2B), TMC1-mCherry puncta were observed at the tips of the shorter rows of stereocilia, but were absent or rarely detected at the tips of the tallest stereocilia. A few puncta were observed along the length of stereocilia suggesting that there may be a population of TMC molecules not located at the site of MET. We also noted that the TMC1-mCherry fluorescence signal was absent from the tips of a few stereocilia in the shorter rows (Figure 2A, arrows). This may be due to decay or bleaching of the fluorophores, or local damage of the stereocilia. Another possibility is that some MET sites lack TMC1, at least transiently, and that the presence of TMC is not required to sustain stereocilia morphology. The pattern of TMC1-mCherry puncta appeared to be indistinguishable between *TMC1-mCherry* mice on either *Tmc1*^{-/-} (Figure 2A) or *Tmc1*^{+/-} backgrounds (Figure S1A), suggesting that the presence of endogenous protein does not affect or preclude the localization of mCherry-tagged TMC1 at stereocilia tips. This pattern of predominant distribution of TMC1-mCherry at the tips of

IHC and OHC stereocilia did not change significantly after exposure to 5 mM BAPTA for 15 min (Figure S2), which is known to disrupt the tip links and abolish MET (Assad et al., 1991). Similar to the observations in cochlear hair cells, TMC1-mCherry puncta localized predominantly at the tips of vestibular hair cell stereocilia (Figures 2C and 2D).

To confirm the TMC1-mCherry localization results, we generated antibodies to detect endogenous protein. The specificity of the antibodies for TMC1 was verified in COS7 cells transfected with constructs encoding TMC1 and TMC2, and in stereocilia from *Tmc1*^{-/-} mice (Figure S3). To detect and localize native TMC1 in cochlear and vestibular stereocilia we used immunostaining based on a protocol (Grati and Kachar, 2011) optimized to detect immunofluorescence signal from low copy-number proteins within the crowded molecular environment of the tip-link insertion site (Kachar et al., 2000). We labeled both mouse and rat inner ear tissue to verify the localization of endogenous TMC proteins in an additional species. Consistent with the localization of TMC1-mCherry, TMC1 immunofluorescence was observed at the tips of the second and third row stereocilia of mouse OHCs, but not at the tips of the tallest row (Figure 2E and 2F). The same pattern of TMC1 immunofluorescence was also observed in rat IHCs (Figure 2G) and OHCs (Figure 2H). Once again, we observed that the immunofluorescence signal was absent in some shorter stereocilia, (Figures 2E – 2H). While this may be because TMC1 can be absent in some stereocilia tips, we cannot exclude that their absence may have been due to epitope masking when labeling a few protein molecules within the densely packed (Kachar et al., 2000) lower tip-link insertion site. TMC1 immunofluorescence puncta were also observed predominantly at the tips of vestibular hair cell stereocilia (Figure 2I).

Distinction between mCherry fluorescence and autofluorescence

It is noteworthy that some autofluorescence was detected in wild type bundles not expressing TMC1-mCherry (Figure S1B). This is likely due to the high gain setting of the system and long exposure times needed to detect the low-abundance TMC1-mCherry. Furthermore, the presence of endogenous auto-fluorescent molecules is exacerbated in stressed or dying tissue (Buschke et al., 2012). To reduce bleaching of TMC1-mCherry and TMC2-AcGFP and limit autofluorescence we performed rapid dissection and fixation. The residual autofluorescence signals, which were clearly much lower in number compared to TMC1-mCherry signal (Figure S1A), were likely the result of debris deposited on the stereocilia surface during dissection of the tissue. The distinction between TMC1-mCherry signal and background autofluorescence was clearly evident when we examined organ of Corti tissue from *Tmc1-mCherry* line 3 mice. Consistent with X-linked inactivation of the *Tmc1-mCherry* transgene, we observed a mosaic expression of TMC1-mCherry fluorescence in OHCs (Figure 3A and 3B) and IHCs (Figure 3C and 3D) of female mice from this line. A similar expression pattern was previously described for a *Myo7a* transgene inserted in the X-chromosome (Prosser et al., 2008). Quantifying the number of fluorescence puncta within hair bundles of *Tmc1-mCherry* line 3 mice, we found that some bundles showed puncta predominantly at the tips of stereocilia of the second and shorter rows (Figure 3A and 3B). The average number of puncta per bundle was 44.8 ± 6 ($n=6$ cells). The other bundles (Figure 3A and 3B, asterisks) showed a lower number (7.2 ± 3.5) of randomly distributed puncta per bundle ($n= 5$ cells), which we assume are due to background

fluorescence. Matching this mosaic pattern of expression of TMC1-mCherry, a mosaic pattern of FM1-43 dye uptake was also observed in P10 cochlear hair cells from line 3 female mice (Figure 3E–G). This was consistent with the large variability in ABR thresholds measured among these mice (Figure 1B).

Localization of TMC2

Similar to TMC1-mCherry, TMC2-AcGFP expressed in *Tmc2-AcGFP* transgenic mice on a *Tmc2*^{-/-} background was also observed in stereocilia as diffraction-limited puncta (Figures 4A–4E). Consistent with the reported spatiotemporal expression of *Tmc2* mRNA (Kawashima et al., 2011), the expression of TMC2-AcGFP in auditory hair cells is transient and disappears as the hair cells mature. To assess the temporal expression during organ of Corti development we focused our analyses to the mid-apical turn of the cochlea, i.e. 30 – 50% from the apex of the cochlea. In IHCs at P4 TMC2-AcGFP fluorescence puncta were localized to the tips of the second and shorter rows of stereocilia and absent from the tips of the tallest row (Figure 4A). Some puncta were also randomly distributed along the stereocilia, distant from the site of MET (Figure 4A). Similar to TMC1-mCherry, we also noted that the TMC2-AcGFP fluorescence signal was absent from the tips of some stereocilia in the shorter rows (Figure 4A, arrows). Localization of TMC2-AcGFP puncta at the tips of stereocilia was also observed in vestibular hair cells (Figure 4B and 4C). However, when compared to cochlear hair cells, greater variations in both the expression level and pattern of distribution of TMC2-AcGFP puncta were observed between stereocilia bundles of different vestibular hair cells, with much larger numbers of puncta present along the length of stereocilia in some cells (Figure 4D and 4E). These differences may be correlated with variations in the type, developmental stage, or both, of the different hair cells in the vestibular sensory epithelia, or may underlie previously unrecognized functional variations between them. Alternatively, they may be the result of transgene over-expression. Immunofluorescence using antibodies specific for TMC2 (Figure S3) in rat inner ear tissue confirmed localization of TMC2 at the tips of stereocilia in IHCs, OHCs and vestibular hair cells (Figures 4F–4H). The observation of stereocilia tip localization of TMC2 in rat cochlear hair cells as late as P15 (Figures 4F and 4G) may be due to differences in the time course of *Tmc2* expression in rat hair cells compared with mouse hair cells.

Spatial and temporal colocalization of TMC1 and TMC2

We next investigated the temporal expression and extent of colocalization of TMC1-mCherry and TMC2-AcGFP during postnatal development in stereocilia of mice expressing both transgenes on a null *Tmc1*^{-/-}; *Tmc2*^{-/-} background (Figures 5, Figure S4, S5 and S6). The earliest that we could consistently detect TMC1-mCherry or TMC2-AcGFP in auditory hair cell stereocilia was at P2 (Figure 5A), when TMC2-AcGFP signal was quite evident. By P3 both TMC1-mCherry and TMC2-AcGFP fluorescent puncta were abundant and localized along the length of stereocilia as well as at the tips, sometimes overlapping (Figure 5A). At P7, TMC2-AcGFP puncta were less evident in OHC stereocilia (Figure S4) but both TMC1-mCherry and TMC2-AcGFP puncta were equally present at stereocilia tips of IHCs (Figure 5A). At P10, TMC2-AcGFP puncta also disappeared from IHC stereocilia, while TMC1-mCherry puncta persisted at stereocilia tips of both IHCs (Figure 5A) and OHCs (Figure S4).

To examine the extent of overlap of localization of TMC1 and TMC2, we analyzed confocal images of IHCs at P7, where both TMC1-mCherry and TMC2-AcGFP were equally abundant (Figure 5A and B). The TMC1-mCherry and TMC2-AcGFP puncta were first identified as local, high-intensity regions (maxima) in the image, using a custom written code in MATLAB®. At each of the identified local maxima, the center of mass of image intensity under a disc-shaped mask roughly the size of the point spread function (5 pixel radius) was then computed to obtain the centroids of each punctum (Figure 5B). The distance between the computed centroid of each TMC1-mCherry punctum and its closest TMC2-AcGFP punctum was used as a measure of separation between puncta. A histogram of the frequency distribution of puncta as a function of their distance to their closest neighbor is shown in Figure 5C. Approximately 25 % of the fluorescent TMC1-mCherry puncta had a TMC2-AcGFP punctum that was within a 30 nm radius, and thus potentially part of the same molecular aggregate or complex (number of puncta = 709, number of cells = 12). Similar results were observed when plotting the frequency of TMC2-AcGFP puncta as a function of the distance to their closest TMC1-mCherry puncta (Figure S5A). Many of the overlapping TMC1-mCherry and TMC2-AcGFP puncta localize to the tips of the second row and shorter stereocilia (Figure 5B, arrows).

We next wanted to determine whether TMC1 and TMC2 compete with each other as interchangeable subunits of a heteromeric aggregate. To do this, we first calculated the intensities of each punctum by integrating the pixel-intensity within a point spread function sized-disc (5 pixel radius, pixel size = 30 nm). We then plotted the fluorescence intensities of each TMC1-mCherry punctum as a function of the distance to its closest TMC2-AcGFP neighbor (Figure 5D). The average intensity of TMC1-mCherry puncta that had a TMC2-AcGFP punctum neighbor within 30 nm was 5.86 ± 2.1 , in arbitrary units (number of puncta = 93, number of cells = 10). The average intensity of TMC1-mCherry puncta whose nearest TMC2-AcGFP neighbor was more than 100 nm away was 4.84 ± 1.7 (number of puncta = 331, number of cells = 10). Conversely, we also plotted the fluorescence intensities of the TMC2-AcGFP puncta as a function of the distance of its closest TMC1-mCherry neighbor (Figure S5B). The average intensity of TMC2-AcGFP puncta that had a TMC1-mCherry punctum neighbor within 30 nm was 8.1 ± 3.8 (number of puncta = 93, number of cells = 10). The average intensity of TMC2-AcGFP puncta when the distance to the closest TMC1-mCherry neighbor was more than 100 nm was 7.5 ± 3.9 (number of puncta = 399, number of cells = 10). These data collectively suggest that the amount of each protein was not reduced when both proteins co-existed within a 30 nm range, and potentially as part of the same molecular cluster.

In the vestibular organs, we did not observe temporal expression differences between TMC1-mCherry or TMC2-AcGFP from P3 (earliest point we examined) to adulthood, and both TMC1-mCherry and TMC2-AcGFP showed a higher degree of cell-to-cell variability compared to cochlear hair cells. While most stereocilia bundles expressed both proteins to some degree, some cells showed predominance of either TMC1-mCherry or TMC2-AcGFP (Figure 5E). When both were expressed in the same hair cell, we observed partial overlap of TMC1-mCherry and TMC2 fluorescence at stereocilia tips (Figures 5F). Of note, the fluorescence puncta sometimes appear to be slightly separated (above) the stereocilia tip. This apparent mismatch is the combined result of the differential size of the point spread

function for the fluorophores and for the actin counterstained stereocilia (stereocilia were stained with phalloidin conjugated to AlexaFluor405, whose emission wavelength is much shorter than the emission wavelengths of mCherry or AcGFP nm) with the fact that the stereocilia often have an elongated and thinner beveled tip where the membrane can be slightly pulled away or tented by tension on the tip link (see figure 4E in Kachar et al, 2000). Together, these parameters give the false impression that the TMC fluorescence puncta are separated from the tip of the actin-counterstained stereocilia.

TMC proteins have been reported to interact with PCDH15 isoforms, and PCDH15 also interacts with CDH23 to form the kinociliary links between the tallest stereocilia and the kinocilium (Gillespie et al., 2005; Goodyear et al., 2010; Kazmierczak et al., 2007). Based on this, we looked for localization of TMC1-mCherry and TMC2-AcGFP along the tallest stereocilia in the bundle, but did not detect any enrichment of either protein at this region.

While the stereocilia tip localization of TMC1 and TMC2 support their having a role in mechanotransduction, we next investigated how TMC1-mCherry and TMC2-AcGFP fluorescence intensity compares between hair cell body and stereocilia to explore the possibility for additional roles of these proteins elsewhere in the cell. The level of fluorescence signal from the cell bodies of hair cells expressing TMC1-mCherry and TMC2-AcGFP on a *Tmc1*^{-/-};*Tmc2*^{-/-} background (Figure S6A and S6B, asterisk) was difficult to differentiate from autofluorescence which is also present in neighboring supporting cells that are not believed to express the tagged proteins (Figure S6A and S6B, double asterisks). When we compared fluorescence in the red channel between hair cells from *Tmc1-mCherry* mice and wild type mice (Figure S6C–S6F), a distinct fluorescence signal was detected in the hair cell bodies (Figure S6C–S6F, asterisk) of the transgenics compared to wild type controls under identical image acquisition conditions. This fluorescence likely corresponds to TMC1-mCherry in endocytic or ER-associated vesicles. No enhancement of fluorescence signal was detected in the hair cell basolateral membrane.

Reverse-polarity currents in *Tmc1*^{-/-};*Tmc2*^{-/-} mice

Recently, non-canonical, reverse-polarity MET currents evoked by deflecting the hair bundle in the direction away from the tallest stereocilia (inhibitory) were recorded from hair cells (Beurg et al., 2014; Kim et al., 2013; Marcotti et al., 2014). These reverse-polarity currents have been shown to occur after tip link disruption by the calcium-chelating agent BAPTA (Kim et al., 2013; Marcotti et al., 2014). While their physiological significance and underlying mechanisms are yet to be elucidated, it was suggested that these reverse-polarity currents may be caused by the relocation of the MET channel as a result of tip link disruption, which might allow for its activation by inhibitory stimuli (Barr-Gillespie and Nicolson, 2013). Because the TMC proteins are hypothesized to be associated with MET, we investigated whether these proteins are required for the reverse-polarity MET currents (Beurg et al., 2014; Kim et al., 2013; Marcotti et al., 2014).

We first confirmed the presence of the reverse-polarity MET currents in wild type hair cells following treatment with 5 mM BAPTA (Figure 6A). We next examined our *Tmc1*^{-/-};*Tmc2*^{-/-} double mutants that are verified null alleles (Kawashima et al., 2011) that do not exhibit conventional transduction when stimulated with a glass probe (Figure 1). We

did not detect any conventional transduction upon delivery of a 40 Hz sine wave stimulus using fluid jet simulation. However, a 25 – 50 % increase in the sine wave stimulus amplitude, that in wild type hair cells evoked maximum MET currents, resulted in appearance of the reverse-polarity currents (Figure 6B). Our data is consistent with recent reports that recorded reverse-polarity currents in *Tmc1* and *Tmc2* mutant mice (Beurg et al., 2014; Kim et al., 2013).

Discussion

While earlier studies suggested that TMC1 is involved in molecular trafficking or intracellular regulatory signaling for hair cell differentiation (Marcotti et al., 2006), more recent studies have provided genetic and physiological evidence for a direct role for TMC1 and TMC2 in hair cell MET (Kawashima et al., 2011; Kim et al., 2013; Pan et al., 2013), suggesting that these proteins are components of the MET complex. One of these reports (Pan et al., 2013) further suggests that TMC1 and TMC2 may be components of the pore-forming element, and the varying conductance properties of the channel may be the result of variations in the relative stoichiometry of these proteins in the channel complex. However, an important milestone in corroborating this hypothesis (Liedtke, 2014) is verifying the precise localization of these proteins at the site of MET (Beurg et al., 2009). The current study shows that TMC1 and TMC2 localize to the specific site of MET at stereocilia tips. We addressed this outstanding question by using two different approaches to detect the proteins. First, we generated transgenic mice expressing mCherry-tagged TMC1 and AcGFP-tagged TMC2. Second, we generated antibodies specific for native TMC1 and TMC2 that we used to label mouse and rat inner ear tissue.

Mice expressing both TMC1-mCherry and TMC2-AcGFP on a *Tmc1*^{-/-};*Tmc2*^{-/-} background showed normal vestibular phenotypes, normal hearing thresholds, and normal whole-cell MET currents within the ranges reported for mice segregating different numbers of wild type alleles of endogenous *Tmc1* and *Tmc2* (Pan et al., 2013). These observations demonstrate that the fluorophore-tagged proteins are functional, properly temporally expressed, and targeted to their site of function.

Our spatiotemporal characterization of TMC1 and TMC2 localization in cochlear hair cells provides insights into the intricate and complex nature of MET currents. In the cochlea at P1, neither TMC1-mCherry nor TMC2-AcGFP is detectable in the stereocilia. By P3 both are abundantly expressed along the length and at the tips of stereocilia. The overall expression of both proteins then declines until about P7, with localization now predominantly at the tips of stereocilia, and a much smaller population of TMC puncta still present along the stereocilia. TMC2-AcGFP expression declines until it virtually disappears by P10, while TMC1-mCherry remains at stereocilia tips through to adulthood. The observed spatiotemporal refinement of TMC localization is reminiscent of the pruning of extracellular stereociliary links and, in particular, lateral links and ankle links, which are present in early postnatal hair bundles but progressively disappear, leaving only tip-links and top connectors in mature hair cells (Goodyear et al., 2005; Waguespack et al., 2007). Furthermore, the developmentally correlated changes in TMC1-mCherry and TMC2-AcGFP localization are consistent with the reported spatiotemporal expression of *Tmc1* and *Tmc2*

mRNA (Kawashima et al., 2011), as well as the acquisition of MET in mouse cochlear hair cells (Lelli et al., 2009). In cochlear hair cells, the TMC proteins were rarely detected at the tips of the tallest row of stereocilia, where functional MET channels are thought to be absent. In vestibular organs, both TMC1-mCherry and TMC2-AcGFP localize to stereocilia tips of mature hair cells showing a cell-to-cell variability in the degree of co-localization of these proteins. Some hair cells show more TMC1 while others show more TMC2. The localization pattern of the fluorophore-tagged TMC1 and TMC2 was confirmed in stereocilia from mice and rats by immunofluorescence detection of endogenous proteins using antibodies specific to TMC1 or TMC2.

We observed a variable number of TMC1-mCherry and TMC2-AcGFP puncta along the length of all mature hair cell stereocilia, which may be due to increased copy number of the proteins in the transgenic mice. However, another possibility is that hair cells retain a pool of TMC proteins along the stereocilia plasma membrane that are actively trafficking or have a yet-to-be-determined function. That we were able to measure reverse-polarity MET currents recently reported by several groups (Barr-Gillespie and Nicolson, 2013; Kim et al., 2013; Marcotti et al., 2014) in our double homozygous null mice (*Tmc1*^{-/-};*Tmc2*^{-/-}), confirms that neither TMC1 nor TMC2 is required for these currents. It is worth noting that we do not detect enrichment of TMC1 or TMC2 along the taller stereocilia contacting the kinocilium where PCDH15 is concentrated, in either developing cochlear hair cells or in vestibular hair cells (Kazmierczak et al., 2007). This suggests that interaction of TMC1/2 with PCDH15 is limited to the site of MET at the tips of stereocilia and does not involve kinociliary links. Inconsistent with our data, a recent attempt to localize TMC1 by immunofluorescence using an antigen retrieval method in wild type mice (Beurg et al., 2015) showed immunoreactivity along the length of the stereocilia, at the tips of the tallest rows of stereocilia, and in the kinocilium - sites where no mechanotransduction is thought to occur.

There is currently no direct data on molecular-level interactions of TMC1 and TMC2. Distinct putative single channel conductances recently reported from wild type IHCs (Pan et al., 2013), led the authors to propose that variations in the stoichiometry of TMC1 and TMC2 might explain tonotopic gradients in the conductance properties of the MET channel. Our localization study provides evidence that TMC2 is only transiently present in stereocilia of cochlear hair cells and thus might not contribute to tonotopic gradients in channel properties (Pan et al., 2013) in mature hair bundles. However, different conductance levels can arise from differential abilities of TMC1 and TMC2, alone or together, to interact with other proteins that affect single-channel MET conductance (Beurg et al., 2014) or simultaneous gating of multiple MET channels in the same complex on a single stereocilium, or different channel complexes on different stereocilia.

Our results also show that when both proteins are expressed at about the same levels, as in IHC stereocilia at P7, only ~25 % of TMC1-mCherry puncta have a TMC2-AcGFP punctum located within a 30 nm radius, and therefore potentially within the same molecular complex or cluster. The remaining puncta were randomly dispersed along the stereocilia. It is possible that TMC1 and TMC2 proteins traffic to the stereocilia membrane as independent clusters or homo-oligomers, and co-accumulate in the limited space at the stereocilia tips by interacting

with other MET components such as PCDH15 (Maeda et al., 2014). This interpretation is supported by our observation that the fluorescence intensity signal emitted by either TMC1-mCherry or TMC2-AcGFP was on average the same regardless of whether the puncta were within interacting distance (<30 nm) or not (>100 nm). This observation may indicate that the presence of one TMC does not exclude the presence of the other at the same locus. It may also indicate that the quantities of TMC1 and TMC2 do not vary whether or not the other is present. One could interpret this to argue against a role for these proteins as pore-forming elements of the MET channel (Pan et al., 2013).

In our current study localizing TMC1 and TMC2 to the site of canonical MET in hair cell stereocilia strongly supports the hypothesis that they are members of the MET channel complex (Schematic model in Figure 7). Whether they are in fact the MET channel, or non-pore-forming subunits/accessory proteins modulating the kinetics of gating, channel properties, stability, or subcellular targeting of the actual channel, is yet to be conclusively established. Association of TMC1 and TMC2 with other MET proteins to form a stable complex may explain TMC1 enrichment at stereocilia tips even after tip link disruption by BAPTA. Other proteins, such as PCDH15 and TMIE, which were recently shown to interact with TMC proteins (Beurg et al., 2015; Fuchs, 2015; Maeda et al., 2014) and TMHS/LHFPL5 identified as an MET channel accessory component (Xiong et al., 2012) may contribute to the spatiotemporal distribution of TMC1 and TMC2 in stereocilia. Similar to TMC, PCDH15 remains at stereocilia tips following BAPTA treatment (Indzhykulia et al., 2013).

Experimental Procedures

Generation of Transgenic Mice

We used bacterial artificial chromosomes (BACs) encoding mouse *Tmc1* or *Tmc2* genes. *Details of the BAC and procedures for their modification, purification and injection into mouse eggs to generate the transgenic mice, as well as backcrossing onto mice segregating targeted deletion alleles of Tmc1 and Tmc2, are fully described in the Supplemental Experimental Procedures.* Founder mice and offspring carrying the BAC transgenes were identified by PCR analysis of genomic DNA isolated from tail biopsies. *All animal protocols and procedures were approved by a National Institutes of Health Animal Care and Use Committee.*

Hair Cell Electrophysiology

Whole-cell, tight-seal technique was used to record mechanotransduction currents from postnatal day P3 – P8 mice by deflecting the hair bundles of IHCs and OHCs using a stiff glass probe. To measure reverse polarity currents, hair bundles were mechanically stimulated with a fluid jet system. The position of the stimulating pipette was adjusted to elicit a maximal MET current. All experiments were performed at room temperature. Details provided in Supplemental Experimental Procedures.

Detection of TMC1-mCherry and TMC2-AcGFP and immunofluorescence microscopy

Inner ear tissue from mice expressing TMC1-mCherry and/or TMC2-AcGFP was dissected and mounted between slide and coverslip and viewed in a *Nikon inverted fluorescence microscope, outfitted with a spinning disk confocal scan head, 100× Apo TIRF 1.49 N.A. objective, and an EM-CCD camera. NIS-Elements imaging software was utilized for image acquisition and analysis.*

For immunofluorescence wild type mice and rat tissue was labeled using polyclonal antibodies against mouse TMC1 (PB277 and PB612) and mouse TMC2 (PB361). See Supplemental Information for further details.

Supplementary Material

Refer to Web version on PubMed Central for supplementary material.

Acknowledgments

We thank Elizabeth Wilson, James McGehee and Patrick Diers for mouse management. Work was supported by NIH intramural research funds Z01-DC000002 (B.K.) and Z01-DC000060 (A.J.G.). B. Pan and J. R. Holt were supported by NIH/NIDCD RO1-DC013521.

References

- Assad JA, Shepherd GM, Corey DP. Tip-link integrity and mechanical transduction in vertebrate hair cells. *Neuron*. 1991; 7:985–994. [PubMed: 1764247]
- Barr-Gillespie PG, Nicolson T. Who needs tip links? Backwards transduction by hair cells. *J Gen Physiol*. 2013; 142:481–486. [PubMed: 24127528]
- Beurg M, Fettiplace R, Nam JH, Ricci AJ. Localization of inner hair cell mechanotransducer channels using high-speed calcium imaging. *Nat Neurosci*. 2009; 12:553–558. [PubMed: 19330002]
- Beurg M, Kim KX, Fettiplace R. Conductance and block of hair-cell mechanotransducer channels in transmembrane channel-like protein mutants. *J Gen Physiol*. 2014; 144:55–69. [PubMed: 24981230]
- Beurg M, Xiong W, Zhao B, Muller U, Fettiplace R. Subunit determination of the conductance of hair-cell mechanotransducer channels. *Proceedings of the National Academy of Sciences of the United States of America*. 2015; 112:1589–1594. [PubMed: 25550511]
- Buschke DG, Squirrell JM, Fong JJ, Eliceiri KW, Ogle BM. Cell death, non-invasively assessed by intrinsic fluorescence intensity of NADH, is a predictive indicator of functional differentiation of embryonic stem cells. *Biol Cell*. 2012; 104:352–364. [PubMed: 22304470]
- Fuchs PA. How many proteins does it take to gate hair cell mechanotransduction? *Proceedings of the National Academy of Sciences of the United States of America*. 2015; 112:1254–1255. [PubMed: 25617369]
- Gale JE, Marcotti W, Kennedy HJ, Kros CJ, Richardson GP. FM1-43 dye behaves as a permeant blocker of the hair-cell mechanotransducer channel. *The Journal of neuroscience : the official journal of the Society for Neuroscience*. 2001; 21:7013–7025. [PubMed: 11549711]
- Gillespie PG, Dumont RA, Kachar B. Have we found the tip link, transduction channel, and gating spring of the hair cell? *Current opinion in neurobiology*. 2005; 15:389–396. [PubMed: 16009547]
- Goodyear RJ, Forge A, Legan PK, Richardson GP. Asymmetric distribution of cadherin 23 and protocadherin 15 in the kinociliary links of avian sensory hair cells. *The Journal of comparative neurology*. 2010; 518:4288–4297. [PubMed: 20853507]
- Goodyear RJ, Marcotti W, Kros CJ, Richardson GP. Development and properties of stereociliary link types in hair cells of the mouse cochlea. *J Comp Neurol*. 2005; 485:75–85. [PubMed: 15776440]

- Grati M, Kachar B. Myosin VIIa and sans localization at stereocilia upper tip-link density implicates these Usher syndrome proteins in mechanotransduction. *Proceedings of the National Academy of Sciences of the United States of America*. 2011; 108:11476–11481. [PubMed: 21709241]
- IndzhukulianAASpanyan R, Nelina A, Spinelli KJ, Ahmed ZM, Belyanseva IA, Friedman TB, Barr-Gillespie PG, Frolenkov GI. Molecular remodeling of tip links underlies mechanosensory regeneration in auditory hair cells. *PLoS Biol*. 2013; 11(6):1001583.
- Kachar B, Parakkal M, Kurc M, Zhao Y, Gillespie PG. High-resolution structure of hair-cell tip links. *Proceedings of the National Academy of Sciences of the United States of America*. 2000; 97:13336–13341. [PubMed: 11087873]
- Kawashima Y, Geleoc GS, Kurima K, Labay V, Lelli A, Asai Y, Makishima T, Wu DK, Della Santina CC, Holt JR, et al. Mechanotransduction in mouse inner ear hair cells requires transmembrane channel-like genes. *J Clin Invest*. 2011; 121:4796–4809. [PubMed: 22105175]
- Kawashima Y, Kurima K, Pan B, Griffith AJ, Holt JR. Transmembrane channel-like (TMC) genes are required for auditory and vestibular mechanosensation. *Pflugers Arch*. 2014
- Kazmierczak P, Sakaguchi H, Tokita J, Wilson-Kubalek EM, Milligan RA, Muller U, Kachar B. Cadherin 23 and protocadherin 15 interact to form tip-link filaments in sensory hair cells. *Nature*. 2007; 449:87–91. [PubMed: 17805295]
- Kim KX, Beurg M, Hackney CM, Furness DN, Mahendrasingam S, Fettiplace R. The role of transmembrane channel-like proteins in the operation of hair cell mechanotransducer channels. *J Gen Physiol*. 2013; 142:493–505. [PubMed: 24127526]
- Kurima K, Peters LM, Yang Y, Riazuddin S, Ahmed ZM, Naz S, Arnaud D, Drury S, Mo J, Makishima T, et al. Dominant and recessive deafness caused by mutations of a novel gene, TMC1, required for cochlear hair-cell function. *Nat Genet*. 2002; 30:277–284. [PubMed: 11850618]
- Lelli A, Asai Y, Forge A, Holt JR, Geleoc GS. Tonotopic gradient in the developmental acquisition of sensory transduction in outer hair cells of the mouse cochlea. *Journal of neurophysiology*. 2009; 101:2961–2973. [PubMed: 19339464]
- Liedtke W. A Precisely Defined Role for the Tip Link-Associated Protein TMIE in the Mechano-electrical Transduction Channel Complex of Inner Ear Hair Cells. *Neuron*. 2014; 84:889–891. [PubMed: 25475183]
- Lyon MF. Gene action in the X-chromosome of the mouse (*Mus musculus* L.). *Nature*. 1961; 190:372–373. [PubMed: 13764598]
- Maeda R, Kindt KS, Mo W, Morgan CP, Erickson T, Zhao H, Clemens-Grisham R, Barr-Gillespie PG, Nicolson T. Tip-link protein protocadherin 15 interacts with transmembrane channel-like proteins TMC1 and TMC2. *Proceedings of the National Academy of Sciences of the United States of America*. 2014; 111:12907–12912. [PubMed: 25114259]
- Marcotti W, Corns LF, Desmonds T, Kirkwood NK, Richardson GP, Kros CJ. Transduction without tip links in cochlear hair cells is mediated by ion channels with permeation properties distinct from those of the mechano-electrical transducer channel. *The Journal of neuroscience : the official journal of the Society for Neuroscience*. 2014; 34:5505–5514. [PubMed: 24741041]
- Marcotti W, Erven A, Johnson SL, Steel KP, Kros CJ. *Tmc1* is necessary for normal functional maturation and survival of inner and outer hair cells in the mouse cochlea. *The Journal of physiology*. 2006; 574:677–698. [PubMed: 16627570]
- Marcotti W, van Netten SM, Kros CJ. The aminoglycoside antibiotic dihydrostreptomycin rapidly enters mouse outer hair cells through the mechano-electrical transducer channels. *The Journal of physiology*. 2005; 567:505–521. [PubMed: 15994187]
- Pan B, Geleoc GS, Asai Y, Horwitz GC, Kurima K, Ishikawa K, Kawashima Y, Griffith AJ, Holt JR. TMC1 and TMC2 are components of the mechanotransduction channel in hair cells of the mammalian inner ear. *Neuron*. 2013; 79:504–515. [PubMed: 23871232]
- Prosser HM, Rzadzinska AK, Steel KP, Bradley A. Mosaic complementation demonstrates a regulatory role for myosin VIIa in actin dynamics of stereocilia. *Mol Cell Biol*. 2008; 28:1702–1712. [PubMed: 18160714]
- Sakaguchi H, Tokita J, Muller U, Kachar B. Tip links in hair cells: molecular composition and role in hearing loss. *Curr Opin Otolaryngol Head Neck Surg*. 2009; 17:388–393. [PubMed: 19633555]

- Schwander M, Kachar B, Muller U. Review series: The cell biology of hearing. *J Cell Biol.* 2010; 190:9–20. [PubMed: 20624897]
- Vreugde S, Erven A, Kros CJ, Marcotti W, Fuchs H, Kurima K, Wilcox ER, Friedman TB, Griffith AJ, Balling R, et al. Beethoven, a mouse model for dominant, progressive hearing loss DFNA36. *Nat Genet.* 2002; 30:257–258. [PubMed: 11850623]
- Waguespack J, Salles FT, Kachar B, Ricci AJ. Stepwise morphological and functional maturation of mechanotransduction in rat outer hair cells. *The Journal of neuroscience : the official journal of the Society for Neuroscience.* 2007; 27:13890–13902. [PubMed: 18077701]
- Xiong W, Grillet N, Elledge HM, Wagner TF, Zhao B, Johnson KR, Kazmierczak P, Muller U. TMHS is an integral component of the mechanotransduction machinery of cochlear hair cells. *Cell.* 2012; 151:1283–1295. [PubMed: 23217710]
- Zhao B, Wu Z, Grillet N, Yan L, Xiong W, Harkins-Perry S, Muller U. TMIE Is an Essential Component of the Mechanotransduction Machinery of Cochlear Hair Cells. *Neuron.* 2014; 84:954–967. [PubMed: 25467981]

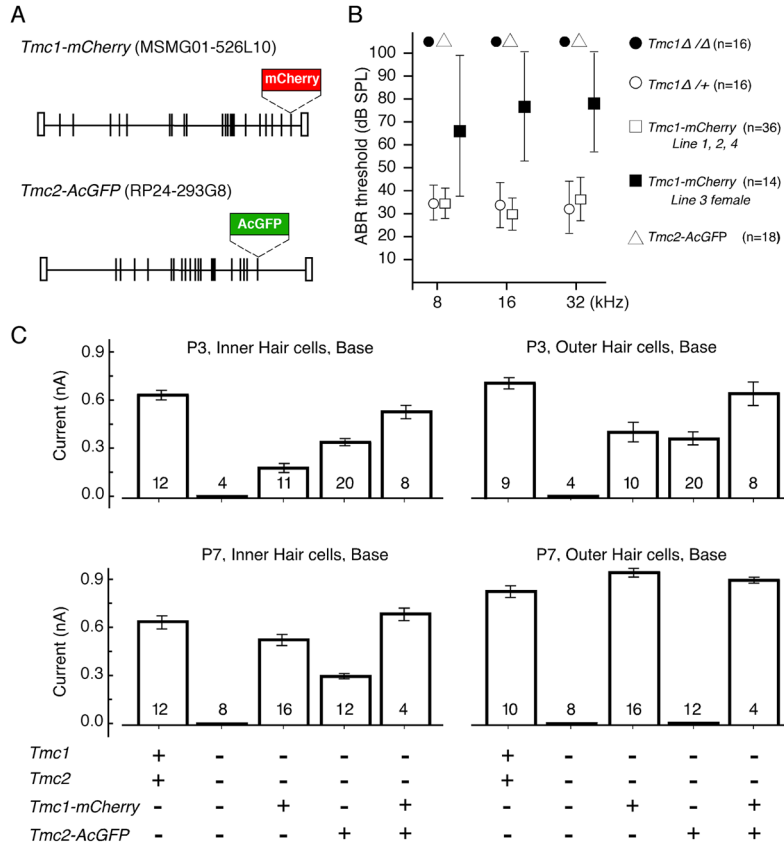


Figure 1. Rescue of hair cell function in *Tmc1*^{-/-};*Tmc2*^{-/-} mice expressing TMC1-mCherry and TMC2-AcGFP

(A) Bacterial artificial chromosome (BAC) transgenes. The stop codons of *Tmc1* or *Tmc2* were replaced with cDNA encoding mCherry or AcGFP, respectively. (B) Mean (±SD) ABR thresholds of 6 to 8-week-old mice for tone-burst stimuli of 8, 16 or 32 kHz. The hearing in mice lacking functional TMC1 was rescued by *Tmc1-mCherry* fully (line 1, 2 and 4) or partially (line 3 females), but not by *Tmc2-AcGFP*. (C) Mean (±SEM) maximal mechanotransduction currents recorded from hair cells excised from mice of the indicated genotypes. Mice with transgenes are on *Tmc1*^{-/-};*Tmc2*^{-/-} background. Transduction currents were evoked using saturating hair bundle deflections and were recorded at -84 mV using the whole-cell, tight-seal technique. Number of hair cells is indicated for each genotype excised from 3 (wild-type), 1 (*Tmc1*^{-/-};*Tmc2*^{-/-}), 3 (*Tmc1-mCherry*), 5 (*Tmc2-AcGFP*) and 2 (*Tmc1-mCherry*:*Tmc2-AcGFP*) P3 mice and 3 (wild type), 2 (*Tmc1*^{-/-};*Tmc2*^{-/-}), 4 (*Tmc1-mCherry*), 5 (*Tmc2-AcGFP*) and 1 (*Tmc1-mCherry*:*Tmc2-AcGFP*) P7 mice.

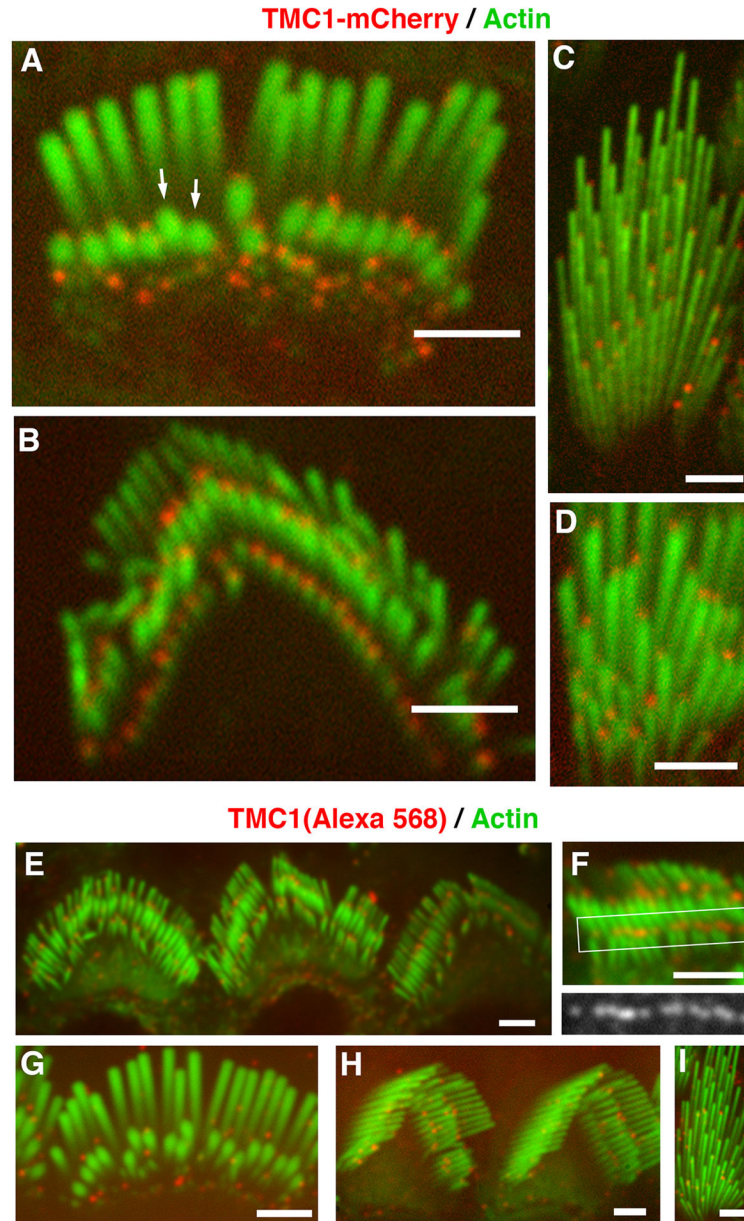


Figure 2. Localization of TMC1-mCherry in hair cell stereocilia

(A) Confocal fluorescence image of IHCs from *Tmc1-mCherry* transgenic mice at P8 (Line 4). TMC1-mCherry (red) localizes predominantly to the tips of the shorter rows of stereocilia, counterstained in green with Alexa Fluor488-phalloidin. (B) TMC1-mCherry (red) distribution in mouse OHC stereocilia (green) at P8 (Line 2). (C and D) TMC1-mCherry (red) localizes to the tips of mouse vestibular stereocilia (green) at P7 (Line 2). (E) Immunofluorescence confocal image of anti-TMC1 antibody (PB277), in P9 mouse OHCs. (F) Close-up view of OHC stereocilia labeled with PB277 shows that TMC1 labeling (red) is present at the tips of second and third rows of stereocilia. Lining up of TMC1 immunofluorescence puncta at the tips of stereocilia is clearly visualized in the boxed region in F, and magnified below. (G and H) Immunofluorescence confocal images of anti-TMC1

antibody (PB277), in P15 rat IHC (G) and OHC (H) stereocilia also shows TMC1 labeling (red) at the tips of second and third rows. (I) TMC1 (red) is consistently detected at the tips of P15 rat vestibular hair cell stereocilia (green) using antibody PB612. [Scale bars: 2 μm]. *See also* Figure S1, S2 and S3.

Author Manuscript

Author Manuscript

Author Manuscript

Author Manuscript

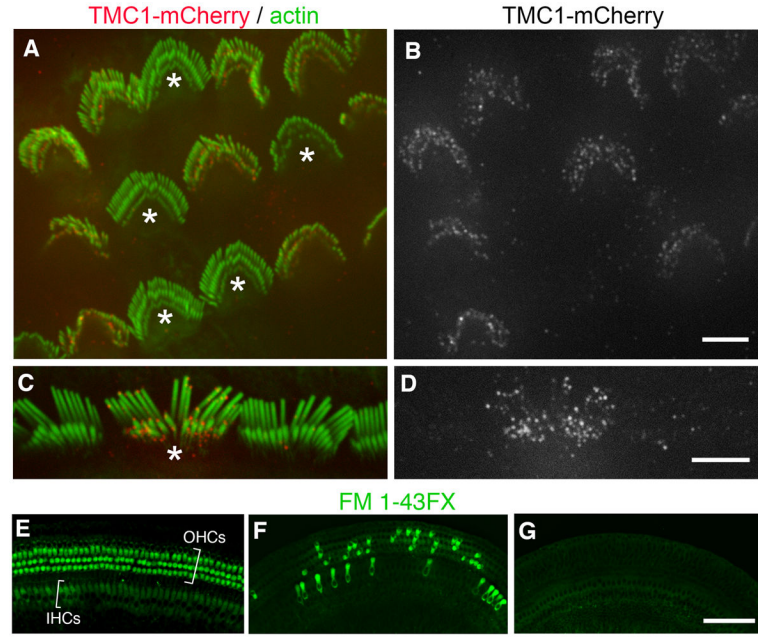


Figure 3. Mosaic expression of TMC1-mCherry in mouse line 3

(A) Confocal image of OHC stereocilia (green) from P10 mice, showing mosaic expression of TMC1-mCherry fluorescent puncta (red). Cells that are not expressing TMC1-mCherry are highlighted with asterisks. (B) Corresponding red channel (TMC1-mCherry) shown in gray. (C) IHC stereocilia (green), showing only one cell (asterisk) expressing TMC1-mCherry. (D) Corresponding red channel (TMC1-mCherry) shown in gray. (E–G) *Confocal images of P10 mouse cochlear hair cells exposed to 5 μM FM1-43 FX. From left to right, IHCs and OHCs from male *Tmc1-mCherry* line 3 mouse, from female *Tmc1-mCherry* line 3 mouse, and from *Tmc1*^{-/-}; *Tmc2*^{-/-} mouse. The *Tmc1-mCherry* line 3 mice were on a *Tmc1*^{-/-}; *Tmc2*^{-/-} background. [Scale bars: A–D = 5 μm; E–G = 100 μm]. See also Figure S1.*

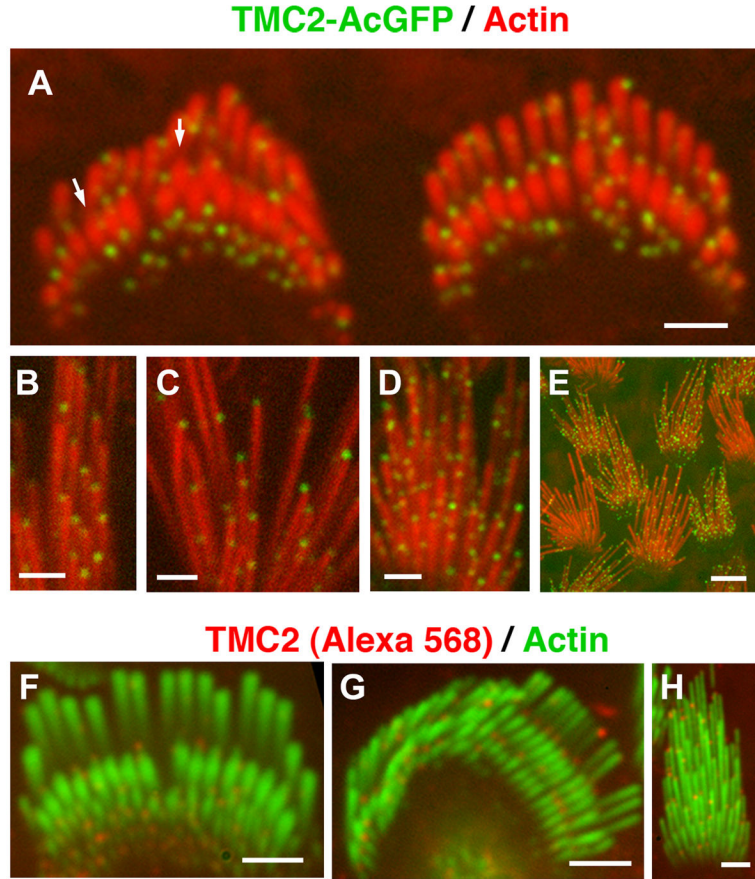


Figure 4. Localization of TMC2-AcGFP in hair cell stereocilia

(A) Confocal images of IHC stereocilia (labeled in red with AlexaFluor568 phalloidin) from *Tmc2-AcGFP* transgenic mice at P4 (Line 4), showing localization of TMC2-AcGFP (green). (B, C) TMC2-AcGFP (green) localizes at the tips of vestibular hair cell stereocilia (red) at P7 (Line 2). (D) In addition to stereocilia tip labeling, some hair bundles at P7 also show abundant TMC2-AcGFP puncta along the length of stereocilia. (E) The expression of TMC2-AcGFP (green) within stereocilia (red) was seen to vary from cell to cell in vestibular organs. (Line 4, P8). (F and G) Immunofluorescence confocal images of rat IHC and OHC stereocilia (green) at P7, showing immunofluorescence of TMC2 (red) using anti-TMC2 antibody PB361. (H) Immunofluorescence staining of TMC2 (red) in stereocilia (green) of rat vestibular hair cells at P3. [Scale bars: A–D, F–H = 2 μ m, E = 5 μ m]. See also Figure S3.

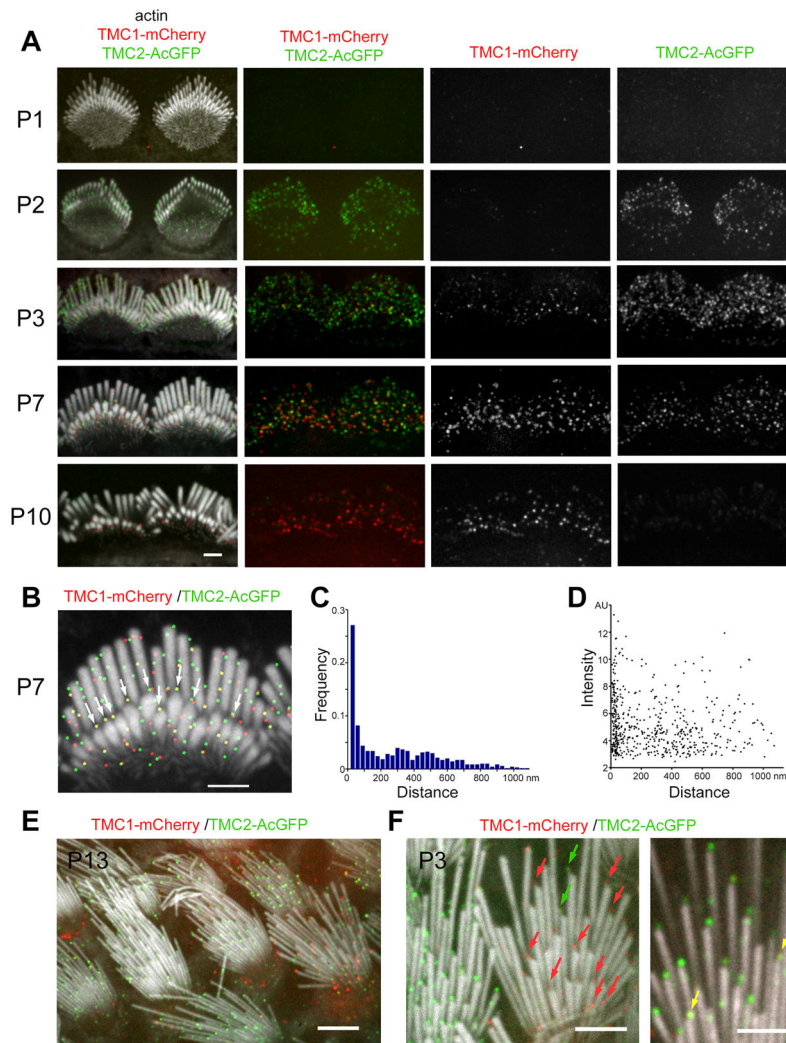


Figure 5. Simultaneous localization of TMC1-mCherry and TMC2-AcGFP in mouse cochlear and vestibular stereocilia

(A) Confocal images of IHC stereocilia from transgenic mice expressing TMC1-mCherry and TMC2-AcGFP at P1, P2, P3, P7 and P10 (*Tmc1-mCherry* Line 2; *Tmc2-AcGFP* Line 3). All cochlear stereocilia bundles are from the mid-apical region of the cochlea (located between 30–50% from the apex of the cochlea). Stereocilia, (labeled with AlexaFluor405 phalloidin) are shown in white (left). Right panels show, respectively, merge of red and green channels, only red channel and only green channel. (B) IHC stereocilia at P7, with calculated centroids for TMC1-mCherry and TMC2-AcGFP puncta represented as red and green dots, respectively, to show relative localization of both signals. (C) Histogram showing the frequency distribution of TMC1-mCherry puncta centroids according to their distance to the centroid of the corresponding closest neighboring TMC2-AcGFP punctum (histogram bin size = 30 nm; number of puncta = 709; number of hair cells = 12). (D) Scatter plot of fluorescence intensity (*in arbitrary units*, AU) of each TMC1-mCherry puncta as a function of the distance to their corresponding closest neighboring TMC2-AcGFP punctum. (E) Confocal images of vestibular hair cells from P13 mice expressing TMC1-mCherry and

TMC2-AcGFP. Stereocilia, labeled with AlexaFluor405 conjugated phalloidin, are shown in white. (*Tmc1-mCherry* Line 2; *Tmc2-AcGFP* Line 4). (F) Close up views of vestibular stereocilia bundles from P3 mouse expressing both TMC1-mCherry and TMC2-AcGFP showing presence of only TMC1-mCherry (red arrows), only TMC2-AcGFP (green arrows), or both (yellow arrows) at stereocilia tips. (*Tmc1-mCherry* Line 2; *Tmc2-AcGFP* Line 4). [Scale bars: A–D, F = 2 μ m; E = 5 μ m]. See also Figure S4–6.

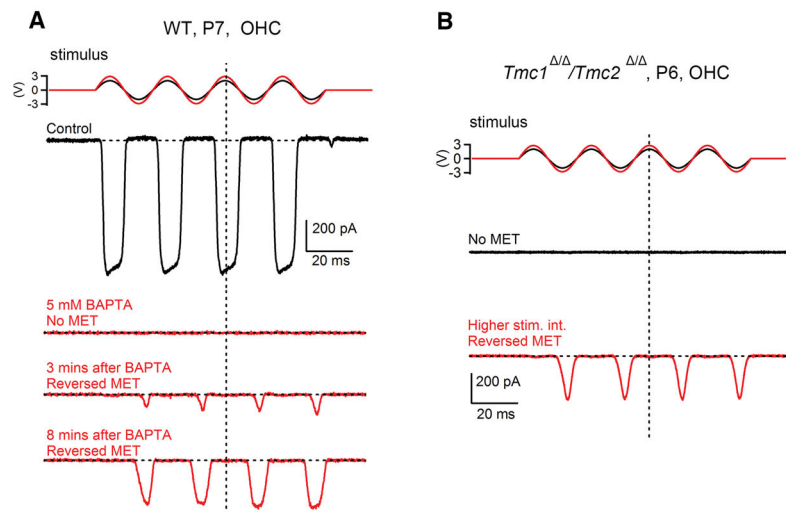


Figure 6. Reverse-polarity currents in WT and $Tmc1^{-/-};Tmc2^{-/-}$ hair cells

(A) Example of MET current (black trace) recorded from a WT outer hair cell (from mid-apical turn of the cochlea, P7 mouse) in response to a sine wave stimulus (black) with a fluid jet device. Upon application of 5 mM BAPTA the MET current of the same cell is abolished (red trace) and followed with the progressive appearance of the reverse polarity currents. (B) Representative MET current recordings from a $Tmc1^{-/-};Tmc2^{-/-}$ outer hair cell. No conventional MET currents were detected during regular stimulation (black trace). A higher stimulus (red sine wave) evoked reverse-polarity currents (red trace). All recordings in panels A and B are averages of 3–8 individual traces (n=5 cells).

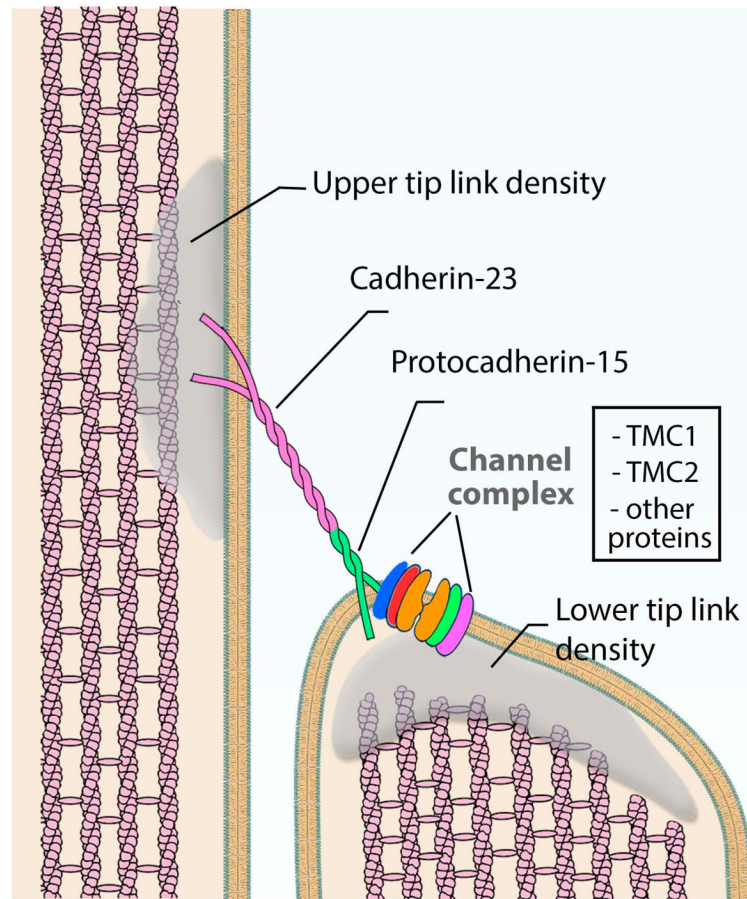


Figure 7. Schematic diagram of stereocilia MET channel complex proteins

Diagram of the stereocilia MET channel complex illustrating the localization of known associated proteins. Localization of TMC1 and TMC2 is consistent with these proteins being components of the complex.